ELSEVIER

Journal of Molecular Structure (Theochem) 632 (2003) 235–246

THEO CHEM

www.elsevier.com/locate/theochem

The sequential Monte Carlo-quantum mechanics methodology. Application to the solvent effects in the Stokes shift of acetone in water

Kaline Coutinho[a], Sylvio Canuto[b,*]

[a]*Universidade de Mogi das Cruzes, CP 411, 08701-970, Mogi das Cruzes, SP, Brazil*
[b]*Instituto de Física, Universidade de São Paulo, CP 66318, 05315-970, São Paulo, SP, Brazil*

Received 2 November 2002

Abstract

The sequential Monte Carlo quantum mechanics methodology is used to obtain the solvent effects on the Stokes shift of acetone in water. One of the great advantages of this methodology is that all the important statistical information is known before running into the costly quantum mechanical calculations. This advantage is discussed not only with respect to the statistical correlation between the different structures generated by the simulation but also in the proper identification of hydrogen bonds in liquids. To obtain the solvent effects in the Stokes shift of the $n-\pi^*$ absorption transition of acetone in water, quantum-mechanical calculations are performed in super-molecular structures generated by NVT Monte Carlo simulation. The statistical correlation between configurations is analyzed using the auto-correlation function of the energy. The largest calculations include one acetone and 170 water molecules. One-hundred INDO/CIS super-molecular calculations are performed for each solvation shell to obtain the statistical average value. The calculated solvatochromic shift of the $n-\pi^*$ absorption transition of acetone in water, compared to gas phase, is $\sim 1310\ cm^{-1}$ in good agreement with the experimental blue shift of $1500 \pm 200\ cm^{-1}$. For the emission of the relaxed excited state, the calculated shift is $\sim 1850\ cm^{-1}$. The total calculated solvent effect on the Stokes shift of acetone in aqueous solution is thus $540\ cm^{-1}$. A detailed analysis of the sampling of the configurations obtained in the Monte Carlo simulation is made and it is shown that all results represent statistically converged values.

Keywords: Monte Carlo-quantum mechanics methodology; Super-molecular calculation; Solvent effects

1. Introduction

Understanding solvent effects is crucial for the correct interpretation of several phenomena that are very common in physics, chemistry and biology [1–4]. The theoretical studies of solvent effects have seen a great development in the recent years. The original ideas of Onsager [5] and Kirkwood [6] have been extended to modern self-consistent-reaction-field or continuum theories [7–19] that have been successful in the study of solvent effects of polar

* Corresponding author. Fax: +55-11-3091-6831.
E-mail address: canuto@if.usp.br (S. Canuto).

0166-1280/03/$ - see front matter © 2003 Elsevier B.V. All rights reserved.
doi:10.1016/S0166-1280(03)00302-6

solutes. A methodology that is now of wide acceptance is the combined use of Quantum Mechanics and Molecular Mechanics method [16–32], the so-called QM/MM methodology. A similar, complementary, approach that has seen increased use and acceptability is the combined use of quantum mechanics with some sort of computer simulation of liquids [30–38]. This is the approach also used in our group where the structures of the liquid are generated by Monte Carlo (MC) computer simulation for subsequent quantum-mechanical (QM) calculations [38–44]. This sequential Monte Carlo quantum mechanics methodology (S-MC/QM) methodology has the advantage that running first the MC simulation gives important statistical information that is advantageously used in the preparation of the subsequent QM calculations [37–40]. For instance, the total number of necessary quantum mechanical calculations can be dramatically reduced if statistically correlated structures are avoided. This can be done systematically using the auto-correlation function of the energy obtained in the simulation [37–40,45].

In this paper we use the S-MC/QM method to study the solvent effects on the Stokes shift (the difference between the absorption and emission transition energies) of acetone. Most carbonyl molecules do not fluoresce. For instance, formaldehyde does not fluoresce. Acetone is the simplest molecule with the hydrogen-bond acceptor C=O group that exhibits a clear emission spectrum. The absorption spectrum of acetone has been the subject of several theoretical studies. In fact, the solvent effect on acetone is one of the first systems that were subjected to a QM/MM methodology for the study of the solvatochromic shift of the $n-\pi^*$ absorption transition [34]. However, the study of the excited states is considerably more scarce. The solvation of electronic excited molecular states has been studied by several groups [43,46–52] but the specific consideration of fluorescence shift is more sparse [43,47,49,51–53]. A fundamental question has to do with the relaxation time of the excited state in the solvent. For the absorption, it is generally assumed that the transition is vertical obeying the Franck–Condon principle. For the emission, instead, the transition initiates in the excited state. If its relaxation time is smaller than its life-time, the excited state may relax the geometry before emitting. If, however, the relaxation is slow the emission will occur in a non-relaxed state. In fact the fluorescence spectrum may be a superposition of instantaneous transitions depending on the solvent relaxation [54]. Acetone is known to have a planar H_2C=O group in the ground state and an out-of-plane in the $n-\pi^*$excited state, similar to formaldehyde. The relaxation of the excited state of formaldehyde has been studied by Levy et al. [46] using molecular dynamics simulation. The solvation dynamics of excited chromophores in acetone as a solvent has been considered [55]. In this paper we study the solvation shift of the $n-\pi^*$ state of acetone both in the absorption and emission and from this we obtain the solvent effect on the Stokes shift, both in the gas phase and in the solvent water environment. We perform a systematic study of the $n-\pi^*$ blue shifts in the absorption and emission of acetone in water where the solvent molecules are explicitly included in the quantum mechanical calculations. We use Monte Carlo simulations to generate structures of the liquid and super-molecular quantum mechanical calculations, with all-valence electrons, to obtain the separate contributions of the different solvation shells to the spectroscopic shift starting from the hydrogen-bonded water molecules. The final result is estimated after extrapolation to the bulk limit. Thus we not only investigate how the solvation shells influence the shift but we also extrapolate our results to obtain our best estimate of the solvatochromic shift of the $n-\pi^*$ absorption and emission transitions of acetone in water, compared to gas phase. It should be remarked that the use of ab initio theories is difficult not only because of the computational effort involved in these large super-molecular calculations but also because we analyze the solvation effects with the size of the super-molecules, and therefore, the use of size-extensive methods is imperative. CIS is a simple theoretical model that includes the advantage of size-extensivity. As most excited states are dominated by single excitations, it is a favorite model for semi-empirical theories [56]. We use the semi-empirical INDO/CIS [56] method that has proven to be a very successful theory for spectroscopy and spectroscopic shifts [36–38] in both polar and non-polar solutes and solvents [37,38,41–44,57,58].

2. Methods of calculation

2.1. Monte Carlo simulation

The Monte Carlo simulation is performed using standard procedures for the Metropolis sampling technique [59] in the canonical ensemble, where the number of molecules N, the volume V and the temperature T are fixed. As usual, periodic boundary conditions in a cubic box [45] are used. In our simulations, we use one acetone molecule plus 450 molecules of water. The volume of the cubic box is determined by the experimental density of the water, $\rho = 0.9966$ g/cm^3 at $T = 25$ °C. The molecules interact by the Lennard–Jones plus Coulomb potential with three parameters for each atom i (ε_i, σ_i and q_i). They are combined to generate the pair-potential parameters by $\varepsilon_{ij} = (\varepsilon_i\varepsilon_j)^{1/2}$ and $\sigma_{ij} = (\sigma_i\sigma_j)^{1/2}$. For the water molecules, we used the SPC potential developed by Berendsen et al. [60]. For the ground and the first excited state of acetone, we use the classical parameters ε_i and σ_i of Gao [34] and the charges are obtained by electrostatic potential fitting in ab initio calculations [61] with HF and CIS/CHELPG (using all single excitations) level, respectively, and 6-311++G(d,p) basis set. The geometry of acetone in the excited state is taken from CASSCF(10,11)/6-311G(d,p) calculations [62]. For the ground state, however, we take into account the small lengthening of the C=O distance that occurs when hydrogen bond is formed with water. We then optimized the geometry of acetone with one water molecule using MP2/6-311++G(d) [63]. This has a small favorable effect in the description of the absorption transition in water, as noted before [33,63]. The geometrical parameters are given in Table 1.We perform the Monte Carlo simulations of acetone in 450 water molecules with the geometry and the classical potential of acetone both in the corresponding ground (Fig. 1a) and first excited (Fig. 1b) states. The parameters of this potential are shown in Table 2. The dipole moment of the excited state is decreased by the $n-\pi^*$ vertical excitation and this leads to the expected blue shift in the absorption. However, in the relaxation of the excited state the dipole moment increases. Thus, the *relaxed* excited state has a larger dipole moment, compared to the equilibrium ground state, of 0.26 D.

Table 1
Geometrical information of the acetone molecule in the ground (Fig. 1a) and first excited (Fig. 1b) states

	Ground state	First excited state
Distances (Å)		
OC_1	1.226	1.355
C_1H_1	1.089	1.084
C_1H_3	1.094	1.089
C_1C_2	1.511	1.521
C_1H_2	1.094	1.087
Angles (degrees)		
OC_1C_2	122.2	112.4
$C_2C_1C_3$	116.8	117.3
Dihedrals (degrees)		
$C_2C_1C_3O$	0	132.4
$OC_1C_2H_1$	−121.2	−170.6
$OC_1C_2H_2$	0	−51.4
$OC_1C_2H_3$	121.2	69.4

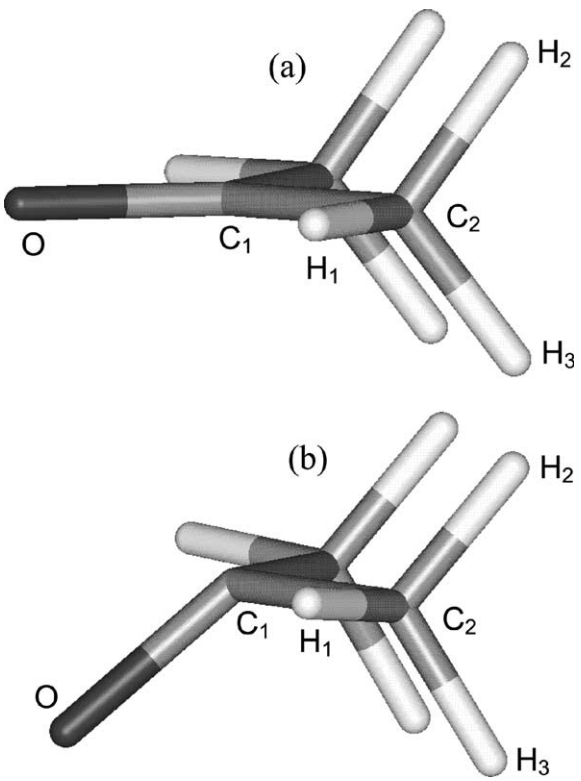

Fig. 1. Illustration of the acetone geometry in the (a) ground and (b) first excited states.

Table 2
Potential parameters for the Lennard–Jones and Coulomb potentials

Atom i	ε_i	σ_i	q_i in ground state	q_i in excited state
O	0.210	2.960	−0.632736	−0.603418
C_1	0.105	3.750	0.778728	0.594348
C_2	0.160	3.910	−0.373880	−0.231246
H_1	0.000	0.000	0.120406	0.036522
H_2	0.000	0.000	0.093321	0.079064
H_3	0.000	0.000	0.087157	0.120195

In the calculation of the pair-wise energy, each molecule interacts with all other molecules within a center of mass separation that is smaller than the cut-off radius $r_c = 11.9$ Å. For separations larger than r_c, we use the long range correction of the potential energy [45]. For the Lennard–Jones potential, the long-range correction is evaluated using the pair radial distribution function and for the Coulomb potential it is evaluated using the reaction field method with dipole interactions (dielectric constant of water = 78.5). The initial configuration is generated randomly, considering the position and the orientation of each molecule. A new MC step is defined by random selecting a molecule and trying to translate it in all the Cartesian directions and also rotate it around a randomly chosen axis. The maximum allowed displacement of the molecules is auto-adjusted after generating 50 configurations to give an acceptance rate around 50%. The maximum rotation angle is fixed in the simulation to $\delta\theta = \pm 15°$. The MC simulation is performed using the DICE [64] program. It involves a thermalization stage of about 5.2×10^6 MC steps followed by an averaging stage of 27×10^6 MC steps. The radial distribution function is also calculated during the averaging stage of the simulation. Structures that are statistically very correlated will not give important additional information. Therefore, we calculate the auto-correlation function of the energy and obtain the interval between configurations of the Monte Carlo simulation that gives statistically new information [37,38,40,65]. This interval is called the correlation step. Essentially, it gives the number of MC steps that statistically uncorrelated configuration can be sampled. For the simulations presented here, we obtain that configurations separated by 27×10^4 MC steps are statistically uncorrelated. Then, the total of 27×10^6 successive configurations generated in the simulation can be drastically reduced to 100 configurations with ~15% of correlation, without compromising the statistical average [37–40,65–67]. Thus, after the simulation, 100 nearly uncorrelated configurations were sampled to be used in further quantum mechanical super-molecular calculations. A detailed discussion on this procedure of sampling configurations will be given below. These 100 configurations will be subjected to quantum mechanical super-molecular calculations.

2.2. Quantum mechanical transition energy calculations

The transition energies are calculated using the ZINDO program [68] within the INDO/CIS [56] model, in the super-molecules generated by the Monte Carlo simulations. The quantum mechanical calculations are then performed for the super-molecular clusters composed of one acetone and all solvent molecules within a particular solvation shell. Each water molecule includes eight valence electrons and the Hartree–Fock wave function is anti-symmetric with respect to the entire solute–solvent system.

The solvatochromic shift in the absorption is given by the difference in the transition energies in the gas phase (ν_0) and in solution (ν_1); i.e. $\Delta\nu_{ab} = \nu_1 - \nu_0$. In the fully relaxed excited state the solvatochromic shift in the emission is given by $\Delta\nu_{em} = \nu_3 - \nu_2$, where ν_2 and ν_3 are the transition energies in the gas phase and in solution, with the solute molecule in the excited geometry (Fig. 2). The Stokes shift in gas phase is given by $\nu_2 - \nu_0$ whereas in the solvent it is

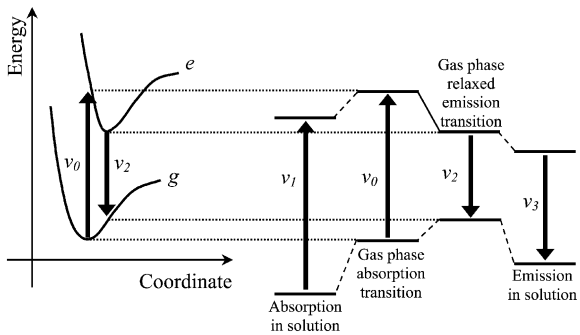

Fig. 2. Illustration of the solvatochromic shift in the absorption ($\Delta\nu_{ab} = \nu_1 - \nu_0$) and the fully relaxed emission ($\Delta\nu_{em} = \nu_3 - \nu_2$).

given by $\nu_3 - \nu_1$. Therefore, the solvent effect on the Stokes shift is given by the difference $\delta = (\nu_3 - \nu_1) - (\nu_2 - \nu_0) = (\nu_3 - \nu_2) - (\nu_1 - \nu_0)$. Thus the difference between the solvatochromic shifts in the absorption and emission gives the solvent effect in the Stokes shift.

The average solvatochromic shift can be obtained as a simple average over L transition energy values

$$\langle E \rangle = \frac{1}{L} \sum_{i}^{L} E_i \tag{1}$$

It is known that independent, or *uncorrelated*, values of E_i generate a normal distribution with a standard deviation and a statistical error of the average. For the hydrogen bonds, in order to have a better statistics, covering the different possible cases with one, two or more water molecules bound to acetone, we use $L = 600$. For the first, second or third hydration shells the value of $L = 100$ is found to be sufficient to give converged values for the solvatochromic shifts. After convergence, increasing L, is immaterial for the average but simply decreases the statistical error.

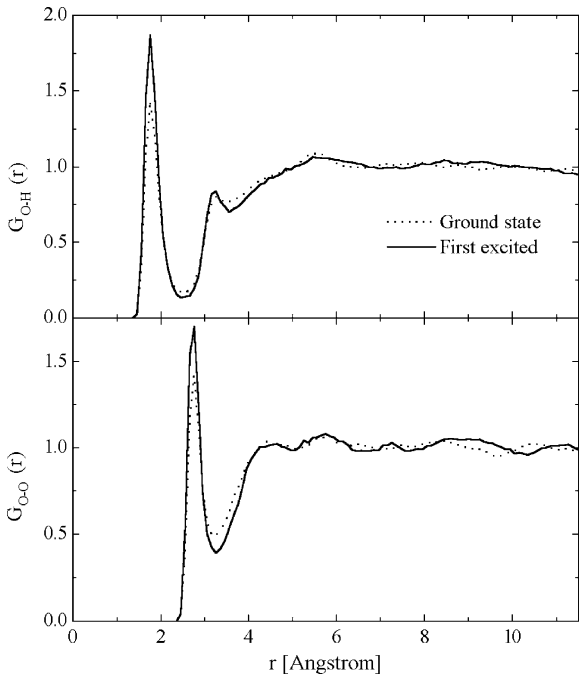

Fig. 3. Radial distribution function between the oxygen atom of acetone (in ground and excited states) and the hydrogen and oxygen atoms of water.

3. Results and discussions

3.1. Hydrogen bond

An important point in the study of computer simulation of liquids is the identification of the hydrogen bonds. We first analyze the pair-wise radial distribution function because it is the conventional and well-known procedure to give the coordination number. The radial distribution function defines also the solvation shells [45]. Fig. 3 shows the radial distribution function between the oxygen of acetone and the hydrogens and the oxygen of water, $G_{O-H}(r)$ and $G_{O-O}(r)$. As it can be seen, there is a hydrogen bond peak that starts at the O–H distance around 1.4 Å and O–O distance around 2.4 Å and ends at the minimum in O–H distance around 2.5 Å and O–O distance around 3.3 Å. Spherical integration of this peak in the $G_{O-O}(r)$ gives a coordination number of 2.2 water molecules in the ground state of the acetone and 2.4 in the first excited state. The uncertainty associated with this procedure is that it cannot be assured that all nearest-neighbor structures involved within a distance O–O smaller than the minimum of $G_{O-O}(r)$ (3.3 Å in this case) are indeed associated with hydrogen bonds. Combining this with the O–H distribution gives better results but structures not associated to hydrogen bond may still persist. Alternative procedures have then been suggested [69]. A very efficient way to extract the hydrogen-bonded structures was discussed earlier by Stilinger and Rahman [70–72] and Mezei and Beveridge [73]. They have emphasized the directional and energetic aspects of hydrogen bonds and their usefulness in identifying hydrogen bonds in computer simulation of liquids. Hydrogen bonds are indeed better obtained using the geometric and energetic criteria [70–75]. We consider here a hydrogen bond when the distance between the oxygen atoms of acetone and water is less than the first minimum of the radial distribution function, 3.3 Å, the angle formed between the oxygen atom of acetone and the OH bond of water is less than 40° and the binding energy is at least 2.7 kcal/mol. The selection of the 2.7 kcal/mol for the cut-off limit of the hydrogen bond is obtained from the histogram of the pair-wise energy distribution. Fig. 4 shows

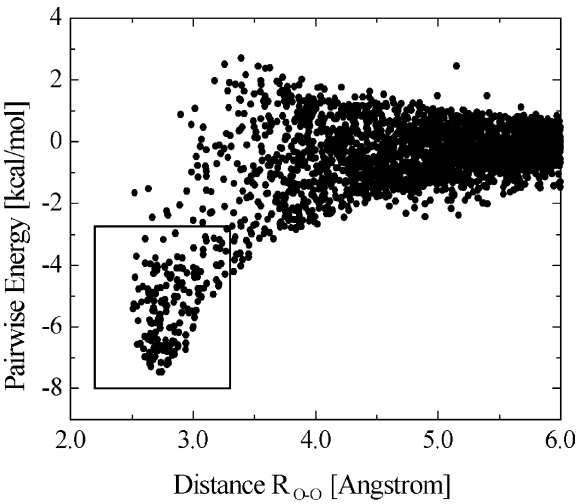

Fig. 4. Pairwise interaction energy between acetone in the ground state and all water molecules. Hydrogen bonds are emphasized.

the pair-wise interaction energy between ground state acetone and water and gives those that are represented by hydrogen bonds. Fig. 5, in complement, shows the histogram of the pair-wise energy distribution. This histogram clearly identifies the hydrogen-bonded structures and show the energy minimum at 2.7 kcal/mol. The geometric–energetic criterion turns out to be a very good way of obtaining hydrogen bonds in liquids [75]. With this, in the 600 MC configurations we find 1004 hydrogen bonds formed between water and acetone in the ground state and 1180 in the first excited state. This gives an average of 1.7 and 2.0 bonds in the ground and excited states, respectively, slightly smaller than the result obtained for the coordination number given by the integration of the first peak of the $G_{O-O}(r)$ radial distribution function. Thus in the excited state the average number of hydrogen bonds is larger by 23% when compared to the ground state. This is a consequence of the dipole moment increase of the relaxed first excited state compared to the ground state. Note that the atomic charge in the oxygen site of the excited state is smaller than that in ground state. The hydrogen bonds formed between acetone and water can now be analyzed in a very detailed form. Table 3 gives the statistics. We find for the ground state of acetone that out of the 600 configurations analyzed, nine make no hydrogen bonds (1.5%) but 213 configurations have one hydrogen bond (35.5%), 343 form two hydrogen bonds (57.2%) and 35 form three hydrogen bonds (5.8%). In the subsequent quantum mechanical calculations these structures can be analyzed separately (Table 3). Calculations of the transition energies are performed on all these complexes with one, two and three water molecules. For instance, 343 INDO/CIS calculations are made with acetone and two water molecules. The resulting average $n-\pi^*$ transition energy is subtracted from the transition of isolated acetone to give the average shift of $816 \pm 37\ cm^{-1}$ for the configurations with two hydrogen bonds. The total blue shift of the HB

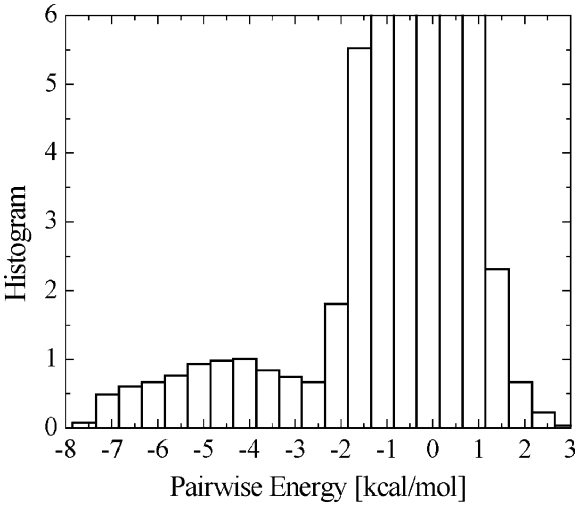

Fig. 5. Pairwise energy distribution and hydrogen bonds between acetone and water.

Table 3
Statistics of the hydrogen bonds formed between acetone in the ground and first excited states and water, and their contribution to the blue shift of the absorption and emission transitions

Number of HB	Ground state		First excited state	
	Occurrence (%)	Shift (cm^{-1})	Occurrence (%)	Shift (cm^{-1})
0	1.5	0	2.0	0
1	35.5	479 ± 36	13.8	623 ± 51
2	57.2	816 ± 37	69.7	1089 ± 27
3	5.8	930 ± 44	14.5	1242 ± 47
Total	100	690 ± 45	100	1025 ± 50

Geometric and energetic criteria are used to sort out a hydrogen bond (see text). The theoretical error bar is the statistical error of the average value.

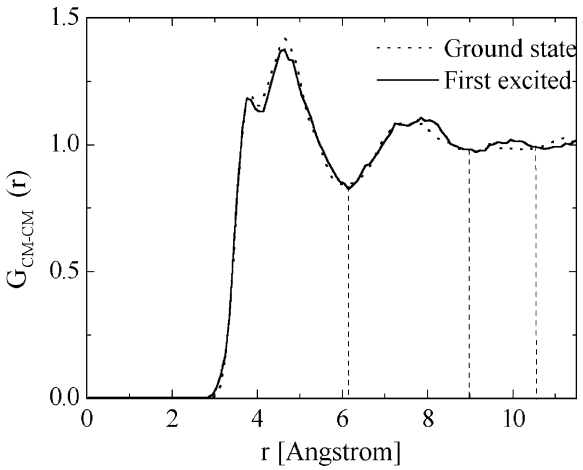

Fig. 6. Radial distribution function between the center-of-mass of acetone (in ground and excited states) and water.

shell is then obtained using a weighted average of the contributions of the configurations with different number of hydrogen bonds. As shown, the total blue shift contribution of the HB solvation in the absorption $n-\pi^*$ of acetone in water is $690 \pm 45\ cm^{-1}$. Similar analysis for the emission gives a total shift of $1025 \pm 50\ cm^{-1}$. The theoretical error bar is the statistical error of the average value.

3.2. Solvation and Stokes shifts

We can now analyze the solvation shifts and the role of the outer shells. Fig. 6 shows the radial distribution function between the center-of-mass of acetone and water. Three solvation shells are discerned. The first shell starts at 2.9 Å ending at 6.15 Å. The second ends at 9.0 Å and a third solvation extends at around 10.7 Å, close to the cut-off radius. Integration of the radial distribution function gives a total of 30, 100 and 170 water molecules from the solute center-of-mass up to the limit of these three shells, respectively, for acetone in both ground and first excited states. Again, we can obtain separately the contribution of each solvation shell. This is of importance because it exposes possible long-range polarization. Table 4 gives the calculated solvatochromic shifts for all solvation shells and summarizes the results. All results shown in Table 4 for the different solvation shells are represented by an average over 100 QM calculations. We shall show later that this is sufficient to give statistically converged values. From the simulation point of view it also means that the configuration space is well represented. To illustrate this important aspect Fig. 7 shows one super-molecular structure corresponding to the first solvation shell (acetone and 30 water molecules) that is sampled from the MC simulation. As 100 of these structures are used to represent the statistics we also show the superposition of all these 100 structures. As can be seen, the configuration space is indeed well represented. The largest calculation is composed of the acetone and 170 water molecules, and gives a calculated blue shift of $1296 \pm 41\ cm^{-1}$ for the absorption and $1837 \pm 60\ cm^{-1}$ for the fully relaxed emission transitions. Most of the solvatochromic shift is obtained by including only the first shell of solvent molecules. However, the results of Table 4 show a small but systematic increase of the solvatochromic

Table 4
Variation of the calculated (INDO/CIS) shifts (in cm^{-1}) of the $n-\pi^*$ absorption and emission transitions of acetone in water with the solvation shells

Solvation shell	N	M	Distance (Å)	Blue shift		Stokes shift
				Absorption	Emission	Stokes shift
First	30	264	6.15	1148 ± 44	1545 ± 65	397 ± 109
Second	100	824	9.00	1251 ± 45	1797 ± 63	546 ± 108
Third	170	1384	10.7	1296 ± 41	1837 ± 60	541 ± 101
Limit	Bulk			1310 ± 40	1850 ± 60	540 ± 100
Experimental [76,77]				1500 ± 200		

N is the number of water molecules included. M is the total number of valence electrons. The theoretical error bar is the statistical error of the average evaluated over 100 super-molecular structures.

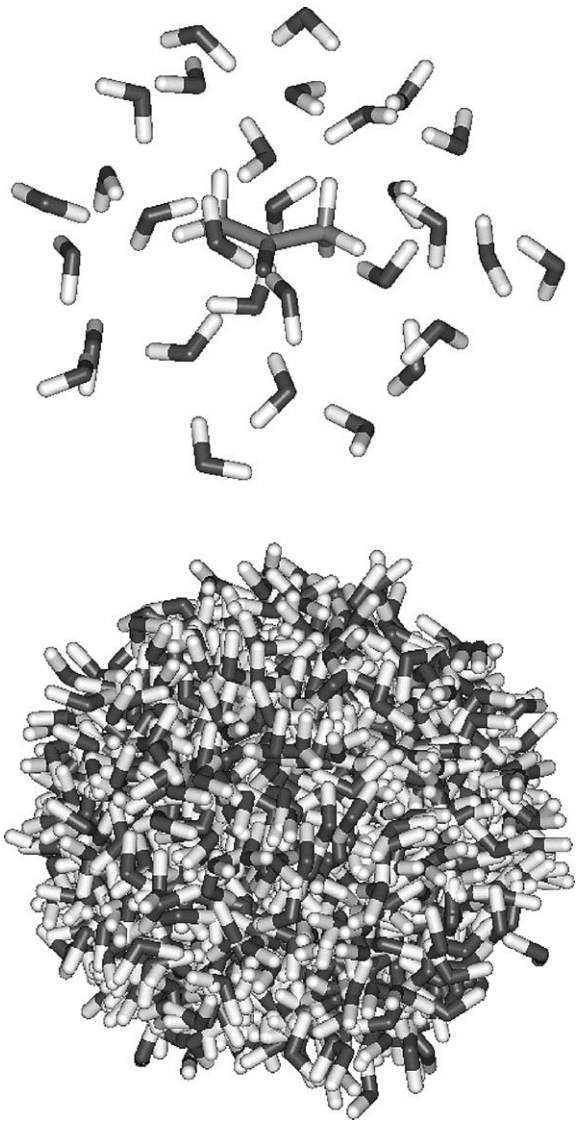

Fig. 7. Illustration of one super-molecular structure corresponding to the first solvation shell and the superposition of all 100 structures sampled from the simulation.

shift due to the second and third shells. It is interesting to note, however, that the solvent effect in the Stokes shift, obtained by the difference in the absorption and emission, is more stable with respect to the number of solvent molecules. The results of Table 4 show that the solvent affects more the separate solvatochromic shifts than the Stokes shift (with respect to the number of solvent molecules included). The monotonic behavior of the calculated energy shift permits an extrapolation of the absorption and emission results to the bulk limit. In doing so we obtain a limiting value of $\sim 1310\ cm^{-1}$ for the absorption and $\sim 1850\ cm^{-1}$ for the emission. This would be our best result of the blue shift of the absorption and the relaxed emission of the $n-\pi^*$ state of acetone in water. It is known experimentally [76,77] that this first absorption transition of acetone suffers a blue shift of $1500 \pm 200\ cm^{-1}$ in water, as compared to the isolated gas phase, in good agreement with our theoretical result. There has been several previous theoretical treatments [30,34,49,52,62,78–82] of this blue shift in the absorption spectrum. A theoretical analysis of the shift in the emission transition of acetone in water was lacking, in spite of the great importance of the fluorescence of acetone [83]. It is of interest to analyze not only the total solvatochromic shifts of acetone in water, in the case of absorption and emission, but also the solvent effect in the Stokes shift. The Stokes shift (i.e. the difference between the absorption and the emission) in water compared to gas phase is obtained here as $540 \pm 100\ cm^{-1}$.

4. Sampling and convergence analysis

The sampling of configurations from statistical simulations is a very important issue and is crucial for the efficiency of statistically-based QM/MM methods. In the S-MC/QM methodology we use the interval of statistical correlation and the statistical inefficiency, to select configurations that give relevant statistical information [23,37–40,66,67]. We have shown previously that this sampling does not compromise the statistical average [37–40]. This is very efficient and gives statistically converged results. In doing so, the subsequent quantum mechanical calculations are performed only on some uncorrelated structures. This is one of the advantages of the sequential procedure of the S-MC/QM, in that all the important MC statistical information is available before running into the QM calculations. As in previous works [37–40,43,44,57,58,75] we calculate the auto-correlation function of the energy, $C(n)$, to obtain the interval

of statistical correlation, using the definition

$$C(n) = \frac{\langle \delta E_i E_{i+n} \rangle}{\langle \delta E^2 \rangle} = \frac{\langle E_i E_{i+n} \rangle - \langle E_i \rangle \langle E_{i+n} \rangle}{\langle E^2 \rangle - \langle E \rangle^2} \qquad (2)$$

where E_i is the energy of a configuration i and E_{i+n} is the energy of the configuration generated n MC steps later. For Markovian processes, it is known that $C(n)$ follows an exponential decay [37,65] $C(n) = \exp(-n/\tau)$ and represents the statistical correlation between configurations separated by n MC steps. Thus, $C(n) = 1$ means that configurations separated by n MC steps are 100% statistically correlated and do not contribute with new statistical information to the average. Analyzing the exponential decay it is easy to see that only with an infinite separation the configurations will be statistically uncorrelated, $C(n = \infty) = 0$. However, in practice the configurations are considered statistically uncorrelated for an interval $n \approx 2\tau$. In the simulations of molecular liquids performed by us, the $C(n)$ was best described by the sum of two exponential functions, $C(n) = c_1 \exp(-n/\tau_1) + c_2 \exp(-n/\tau_2)$, where $\tau_2 \gg \tau_1$. In this case, τ is calculated by integrating $C(n)$ from zero to infinite, then $\tau = c_1\tau_1 + c_2\tau_2 \cong c_2\tau_2$. The same behavior of the auto-correlation function was found by other authors [66,67] in simulations of spin models in a lattice. A complementary and alternative way to obtain statistical correlation is discussed in detail in a previous paper [37].

The auto-correlation function of the energy for the ground state simulation of acetone in water is shown in Fig. 8 (in this figure n is normalized by the number of molecules, 450). We obtain here that the correlation step $2\tau = 270 \times 10^3$ MC steps (from Fig. 8 we have $2\tau = 2 \times 450(0.4 \times 13 + 0.6 \times 485)$]. Using configurations separated by less than this is a waste because it includes configurations that do not contribute to the average. Further, if the simulation is not long enough it will give statistically non-converged results in spite of the large computational effort. Therefore, we select one configuration in each 270×10^3 MC steps and use them to perform QM calculations. This assures that the structures used in the quantum mechanical calculations are statistically relevant and converged values are obtained, as it will be demonstrated below. As the total number of MC

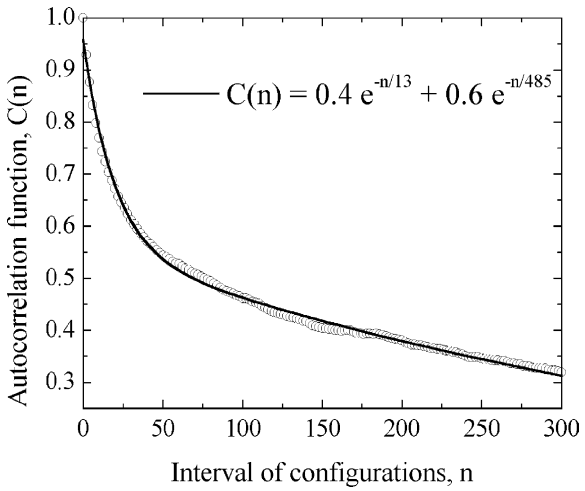

Fig. 8. Calculated auto-correlation function of the energy for the MC simulation of ground state acetone in water.

steps in the simulation was 27×10^6, the averages are then taken over 100 uncorrelated configurations.

It is important now to discuss the convergence of the final results. It is also convenient to show the statistical efficiency obtained with the auto-correlation function of the energy. Fig. 9 shows the histogram and the average solvatochromic shifts of the absorption and emission transitions of acetone in water using the results obtained for the third solvation shell. At this stage it is convenient to analyze the dependence of our calculated average value of

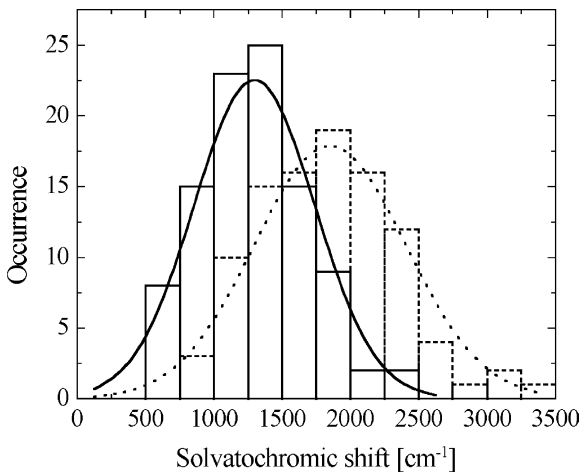

Fig. 9. Histogram showing the statistical convergence of the average value for the absorption and emission shift of acetone in water (results for the third solvation shell).

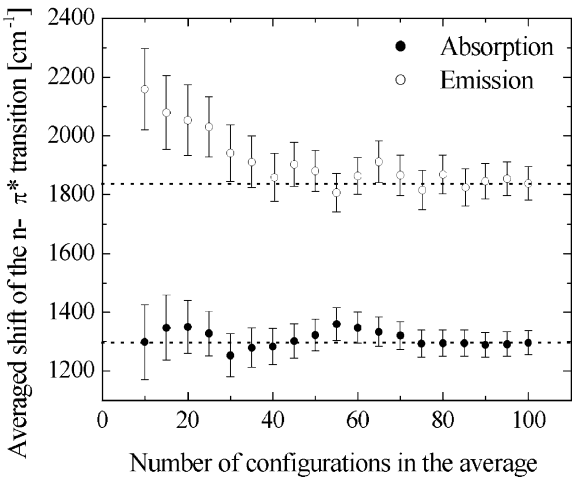

Fig. 10. Convergence of the calculated shifts for the absorption and emission with the number of configurations used.

the solvatochromic shifts on the set of L values used in the calculation. If the sampling is efficient the average value should converge fast and systematically and should be independent [39,40] of the particular choice of the set of MC configurations selected for the QM calculations. The statistical error of the average, however, depends on the total number of uncorrelated configurations (L) used to calculated the average; i.e. on the total size of the simulation. Fig. 10 shows the calculated transition energies for different L. The results clearly demonstrate that the average value has converged after around 80 QM calculations. This is again a demonstration of the efficiency of the use of the auto-correlation function in that only $L \approx 80$ instantaneous values give statistically converged results. Increasing further the number of calculations does not change the average transition energy but, of course, the statistical error σ decreases with increasing L. Thus the use of the interval of the statistical correlation obtained using the auto-correlation function of the energy is a very effective and systematic way to assure statistically converged results with a relatively small number of calculations, because only statistically relevant configurations are included.

5. Summary and conclusions

There has been a large number of theoretical investigations of solvent effects in the absorption spectroscopy but very few theoretical studies are dedicated to the emission process and the Stokes shift. The very systematic and statistically driven S-MC/QM methodology is used to study fluorescence spectroscopy in solution. Using the S-MC/QM methodology the Stokes shift of acetone in water was analyzed using several solvation shells, starting with the hydrogen bonds. An important advantage of this methodology is that all solvent molecules are treated quantum-mechanically. INDO/CIS calculations are performed to obtain the transition energies. To obtain the average, calculations are made on structures generated by the Monte Carlo simulation. These structures are statistically nearly uncorrelated and statistical convergence is demonstrated. The auto-correlation function is used to systematically obtain these structures. A detailed analysis is made of the proper identification and the contribution of the hydrogen bonds. This is again another advantage of performing first the simulation and next the quantum mechanical calculations. Indeed all the statistical information is known after the MC simulation and the distribution is used to proper identify hydrogen bonds in liquids. Next, in the present application, 100 quantum mechanical calculations were made for each of the solvation shells. In the largest calculation we used 100 supermolecular structures composed of one acetone surrounded by 170 water molecules, corresponding to the third solvation shell, extending to 10.7 Å, from the center of mass of acetone. The calculated averages for the hydrogen bond shell and the first three solvation shells give blue shifts for the absorption that are 690 ± 45, 1148 ± 44, 1251 ± 45 and $1296 \pm 41\ cm^{-1}$, respectively. Extending these results to the bulk limit we find a solvatochromic shift in the absorption that amounts to $1310 \pm 40\ cm^{-1}$, in very good agreement with the experimental result of $1500 \pm 200\ cm^{-1}$. In the emission case, we find that these numbers are, respectively, 1025 ± 50, 1545 ± 65, 1797 ± 63 and $1837 \pm 60\ cm^{-1}$ extending to a bulk limit of $1850 \pm 60\ cm^{-1}$. The solvent effect on the Stokes shift is dominated by the first solvation shell. The best result obtained here gives a total solvent effect to the Stokes shift of $540 \pm 100\ cm^{-1}$ for acetone in water.

Acknowledgements

This work has been partially supported by CNPq, CAPES/PROBRAL and FAPESP (Brazil).

References

[1] C. Reichardt, Solvent Effects in Organic Chemistry, Verlag Chemie/Weinheim, New York, 1979.
[2] J. Tomasi, M. Persico, Chem. Rev. 94 (1994) 2027.
[3] C.J. Cramer, D.G. Thrular, Solvent Effects and Chemical Reactions, in: O. Tapia, J. Bertrán (Eds.), Kluwer, Dordrecht, 1996, p. 1. C.J. Cramer, D.G. Thrular, Chem. Rev., 99, 1999, pp. 2161.
[4] P. Ogilby, Acc. Chem. Res. 32 (1999) 512.
[5] L. Onsager, J. Am. Chem. Soc. 58 (1936) 1486.
[6] J.G. Kirkwood, J. Chem. Phys. 2 (1934) 351.
[7] O. Tapia, O. Goscinski, Mol. Phys. 29 (1975) 1653.
[8] J.L. Rivail, D. Rinaldi, Chem. Phys. 18 (1976) 233.
[9] S. Miertus, E. Scrocco, J. Tomasi, J. Chem. Phys. 55 (1981) 117.
[10] M.M. Karelson, M.C. Zerner, J. Phys. Chem. 96 (1992) 6949.
[11] A. Klamt, G. Schüürman, J. Chem. Soc. Perkins Trans. 2 (1993) 799.
[12] C.J. Cramer, D.G. Truhlar, J. Am. Chem. Soc. 113 (1991) 8305.
[13] E. Cances, B. Mennucci, J. Tomasi, J. Chem. Phys. 107 (1997) 3032.
[14] C. Chipot, D. Rinaldi, J.L. Rivail, Chem. Phys. Lett. 191 (1991) 287.
[15] K.V. Mikkelsen, H. Ågren, H.J.A. Jensen, T. Helgaker, J. Chem. Phys. 89 (1988) 3086.
[16] O. Christiansen, K.V. Mikkelsen, J. Chem. Phys. 110 (1999) 1365.
[17] R. Cammi, J. Tomasi, J. Comput. Chem. 16 (1995) 1449.
[18] M. Svensson, S. Humbel, R.D.J. Froese, T. Matsubara, S. Sieber, K. Morokuma, J. Phys. Chem. 100 (1996) 19357. T. Vreven, B. Mennucci, C.O. Silva, K. Morokuma, J. Tomasi, J. Chem. Phys. 115 (2001) 62.
[19] M. Cossi, G. Scolmani, N. Rega, V. Barone, J. Chem. Phys. 117 (2002) 43.
[20] A. Warshel, M. Levitt, J. Mol. Biol. 103 (1976) 227.
[21] M.J. Field, P.A. Bash, M. Karplus, J. Comp. Chem. 11 (1990) 700.
[22] J. Gao, X. Xia, Science 258 (1992) 631.
[23] K. Coutinho, S. Canuto, Adv. Quantum Chem. 28 (1997) 89.
[24] M.A. Thompson, J. Phys. Chem. 100 (1996) 14494.
[25] J. Gao, C. Alhambra, J. Am. Chem. Soc. 119 (1997) 2962.
[26] R. Cammi, B. Mennucci, J. Tomasi, J. Am. Chem. Soc. 120 (1998) 8834.
[27] J.L. Rivail, J. Mol. Graph. Model 16 (1998) 272.
[28] S. Antonczak, G. Monard, M.F. Ruiz-Lopez, J.L. Rivail, J. Am. Chem. Soc. 120 (1998) 8825.
[29] G. Monard, K.M. Merz, Acc. Chem. Res. 32 (1999) 904.
[30] M.E. Martin, M.L. Sánchez, F.J. Oliveira del Valle, M.A. Aguilar, J. Chem. Phys. 113 (2000) 6308.
[31] R. Iftimie, D. Salahub, D.Q. Wei, J. Schofield, J. Chem. Phys. 113 (2000) 4852.
[32] M.E. Martin, M.L. Sánchez, F.J. Oliveira del Valle, M.A. Aguilar, J. Chem. Phys. 116 (2002) 1613.
[33] J.T. Blair, K. Krogh-Jespersen, R.M. Levy, J. Am. Chem. Soc. 111 (1989) 6948.
[34] J. Gao, J. Am. Chem. Soc. 116 (1994) 9324.
[35] J. Zeng, N.S. Hush, J.R. Reimers, J. Chem. Phys. 99 (1993) 1496.
[36] A. Broo, G. Pearl, M.C. Zerner, J. Phys. Chem. A101 (1997) 2478.
[37] K. Coutinho, S. Canuto, M.C. Zerner, J. Chem. Phys. 112 (2000) 9874.
[38] S. Canuto, K. Coutinho, Int. J. Quantum Chem. 77 (2000) 192.
[39] W.R. Rocha, K. Coutinho, W.B. de Almeida, S. Canuto, Chem. Phys. Lett. 335 (2001) 127.
[40] K. Coutinho, M.J. Oliveira, S. Canuto, Int. J. Quantum Chem. 66 (1998) 249.
[41] S. Canuto, K. Coutinho, D. Trzresniak, Adv. Quantum Chem. 41 (2003) 161.
[42] S. Canuto, D. Trzesniak, K. Coutinho, in: M. Manmohan (Ed.), Current Developments in Atomic, Molecular and Chemical Physics with Applications, Kluwer/Plenum, Dordrecht, 2002, pp. 127–131.
[43] K. Coutinho, S. Canuto, J. Chem. Phys. 113 (2000) 9132.
[44] K.J. de Almeida, K. Coutinho, W.B. de Almeida, W.R. Rocha, S. Canuto, Phys. Chem. Chem. Phys. 3 (2001) 1583.
[45] M.P. Allen, D.J. Tildesley, Computer Simulation of Liquids, Clarendon Press, Oxford, 1987.
[46] M. Levy, D.B. Kitchen, J.T. Blair, K. Krogh-Jespersen, J. Phys. Chem. 94 (1990) 4470.
[47] S. Ten-no, F. Hirata, S. Kato, J. Chem. Phys. 100 (1994) 7443. S. Ten-no, F. Hirata, S. Kato, Chem. Phys. Lett. 214 (1993) 391.
[48] H. Houjou, M. Sakurai, Y. Inoue, J. Chem. Phys. 107 (1997) 5652.
[49] B. Mennucci, R. Cammi, J. Tomasi, J. Chem. Phys. 109 (1998) 2798.
[50] T.D. Poulsen, P.R. Ogilby, K.V. Mikkelsen, J. Chem. Phys. 111 (1999) 2678.
[51] M.L. Sánchez, M.A. Aguilar, F.J. Olivares del Valle, J. Phys. Chem. 99 (1995) 15758.
[52] M. Baba, I. Hanazaki, U. Nagashima, J. Chem. Phys. 82 (1985) 3938.
[53] B.L. van Duuren, Chem. Rev. 63 (1963) 325.
[54] P. Suppan, N. Ghoneim, Solvatochromism, The Royal Society of Chemistry, Cambridge, 1997.
[55] K. Biswas, B. Bagchi, J. Phys. Chem. A 103 (1999) 2495.
[56] J. Ridley, M.C. Zerner, Theor. Chim. Acta 32 (1973) 111.
[57] W.R. Rocha, K.J. de Almeida, K. Coutinho, S. Canuto, Chem. Phys. Lett. 345 (2001) 171.
[58] W.R. Rocha, V.M. Martins, K. Coutinho, S. Canuto, Theor. Chem. Acc. 108 (2002) 31.
[59] N. Metropolis, A.W. Rosenbluth, M.N. Rosenbluth, A.H. Teller, E. Teller, J. Chem. Phys. 21 (1953) 1087.

[60] H.J.C. Berendsen, J.P.M. Postma, W.F. van Gunsteren, J. Hermans, in: B. Pullmam (Ed.), Intermolecular Forces, Reidel, Dordrecht, 1981, p. 331.
[61] M.J. Frisch, G.W. Trucks, H.B. Schlegel, G.E. Scuseria, M.A. Robb, J.R. Cheeseman, V.G. Zakrzewski, J.A. Montgomery Jr., R.E. Stratmann, J.C. Burant, S. Dapprich, J.M. Millam, A.D. Daniels, K.N. Kudin, M.C. Strain, O. Farkas, J. Tomasi, V. Barone, M. Cossi, R. Cammi, B. Mennucci, C. Pomelli, C. Adamo, S. Clifford, J. Ochterski, G.A. Petersson, P.Y. Ayala, Q. Cui, K. Morokuma, D.K. Malick, A.D. Rabuck, K. Raghavachari, J.B. Foresman, J. Cioslowski, J.V. Ortiz, A.G. Baboul, B.B. Stefanov, G. Liu, A. Liashenko, P. Piskorz, I. Komaromi, R. Gomperts, R.L. Martin, D.J. Fox, T. Keith, M.A. Al-Laham, C.Y. Peng, A. Nanayakkara, C. Gonzalez, M. Challacombe, P.M.W. Gill, B. Johnson, W. Chen, M.W. Wong, J.L. Andres, C. Gonzalez, M. Head-Gordon, E.S. Replogle, J.A. Pople, GAUSSIAN 98, Revision A.7, Gaussian Inc., Pittsburgh PA, 1998.
[62] D.W. Liao, A.M. Mebel, M. Hayashi, Y.J. Shiu, Y.T. Chen, S.H. Lin, J. Chem. Phys. 111 (1999) 205.
[63] K. Coutinho, N. Saavedra, S. Canuto, Theochem. J. Mol. Struct. 466 (1999) 69.
[64] K. Coutinho, S. Canuto, DICE: A Monte Carlo Program for Molecular Liquid Simulation, University of São Paulo, 1997.
[65] C. Chatfield, The Analysis of Time Series. An Introduction, third ed., Chapman & Hall, London, 1984.
[66] R. Krätschmer, K. Binder, D. Stauffer, J. Stat. Phys. 15 (1976) 267.
[67] S. Tang, D.P. Landau, Phys. Rev. B 36 (1987) 567.
[68] M.C. Zerner, ZINDO: A semi-empirical program package, University of Florida, Gainesville, FL 32611, 1999.
[69] H. Sato, F. Hirata, J. Chem. Phys. 111 (1999) 8545.
[70] A. Rahman, F.H. Stilinger, J. Chem. Phys. 55 (1971) 3336.
[71] F.H. Stilinger, A. Rahman, J. Chem. Phys. 60 (1974) 1545.
[72] F.H. Stilinger, Adv. Chem. Phys. 31 (1975) 1.
[73] M. Mezei, D.L. Beveridge, J. Chem. Phys. 74 (1981) 622.
[74] W.L. Jorgensen, J. Chandrasekhar, J.D. Madura, R.W. Impey, M.L. Klein, J. Chem. Phys. 79 (1983) 926.
[75] T. Malaspina, K. Coutinho, S. Canuto, J. Chem. Phys. (2002) 117.
[76] W.P. Hayes, C.J. Timmons, Spectrochim. Acta 21 (1965) 529.
[77] N.S. Bayliss, E.G. McRae, J. Phys. Chem. 58 (1954) 1006.
[78] A.H. De Vries, P.Th. van Duijnen, Int. J. Quantum Chem. 57 (1996) 1067.
[79] Y.J. Shiu, M. Hayashi, A.M. Mebel, Y.T. Chen, S.H. Lin, J. Chem. Phys. 115 (2001) 4080.
[80] L. Serrano-Andrés, M.P. Fülscher, G. Karlström, Int. J. Quantum Chem. 65 (1997) 167.
[81] K. Naka, A. Morita, S. Kato, J. Chem. Phys. 110 (1999) 3484.
[82] K. Honma, K. Arita, K. Yamasaki, O. Kajimoto, J. Chem. Phys. 94 (1991) 3496.
[83] M.C. Thurber, R.K. Hamson, Appl. Phys. B 69 (1999) 229.